Optimal Energy Transfer Pipe Arrangement for Acoustic Drill String Telemetry

Lakshmi Sutha Kumar, *Member, IEEE*, Wei Kwang Han, Yong Liang Guan, *Member, IEEE*, Sumei Sun, *Senior Member, IEEE*, and Yee Hui Lee, *Member, IEEE*

***Abstract*—Drill string acoustic telemetry is an effective transmission method to retrieve downhole data. Finite-difference simulations produce the comb-filter-like channel response (patterns of pass bands and stop bands) due to the presence of coupling joints in the metallic drill string. Practical pipes used for drilling deep wells have slight variation in length. The selection and arrangement of downhole pipes is important for improving the transmission efficiency of extensional waves transmitted through the drill string. Downhole drill string channel is studied using the transmission coefficients calculated from the transmission matrix method, and the resultant transfer function produces identical results similar to the finite-difference simulations. Reciprocity of the drill string structure is proved by comparing the pass band responses using the ascend-only (AO) and descend-only pipe arrangements. Transferred energies calculated up to 180 pipes of random length at the end of the drill strings using transmission coefficients for the three different pipe arrangements, namely, AO, descend-then-ascend, and ascend-then-descend (ATD), are compared to find the optimal pipe arrangement for single measurement. For the situations when pipes are distributed in sets, multiple measurements are required. In this paper, two sets of AO and two sets of ATD arrangements are analyzed for multiple measurements. ATD and nxATD arrangements are proposed as optimal pipe arrangements to produce the best possible telemetry performance in terms of optimal acoustic energy transfer via one- and two-way acoustic communication for single and multiple measurements, respectively.**

***Index Terms*—Acoustic telemetry, comb-filter response, drill string, finite-difference time-domain (FDTD) algorithm, pipe periodicity, reciprocity principle, transfer matrix.**

I. Introduction

DEEP subterranean wells are typically drilled using drill strings assembled by pipe elements, which are approximately 10 m long, using heavy threaded tool joints. Communication of information to the surface from downhole sensors of parameters such as pressure, temperature, drilling direction, or formation is desirable. The operator can use this information for navigational purposes, to control the drill bit torque, or to abort the mission, if necessary. Obtaining this capability translates to increased efficiency and substantial reductions in operating cost. Various methods of communicating that have been tried with varying degrees of success include electromagnetic radiation through the ground formation [1], electrical transmission through an insulated cable [2], laser communication through a fiber optic cable [3], pressure pulse propagation through the drilling mud [4], and wave propagation through the metal drill string [5], [6]. The electronic wire line telemetry system utilizes the cables to transmit information from downhole to the surface. It has the advantages of real time, high speed, surface readout, and surface energy supply. However, wire line telemetry is prone to failures caused by the abrasive conditions of the mud and the wear abrasions caused by the rotation of the drill string [7], [8]. The use of special drill pipe and special tool joint connectors substantially increases the cost of the drilling operation. So far, mud-pulse telemetry has been the only commercially successful method. However, attenuation mechanisms in the mud limit the transmission rate to less than 5 b/s. On the other hand, due to the strong dependence of electromagnetic wave propagation properties to the formation's resistivity profile, electromagnetic telemetry is not a popular technique and has very limited applications. Among all, acoustic telemetry is one of the promising techniques that can achieve a reliable and high-rate Logging-While-Drilling (LWD) telemetry [9], [10].

The idea of acoustic wave transmission through the drill string was initially proposed in 1948 by Sun Oil Company, who also performed the first field test to measure the acoustic attenuation of the drill string [11]. Systematic analysis of acoustic wave propagation in the drill string was carried out by Barnes and Kirkwood [5] and Drumheller [6]. Several patents were later issued on devices based on this telemetry technique [11], [12]. Pipe periodicity of the drill string structure introduces important impacts for wave propagation. One such impact is the pass bands and stop bands in the frequency spectrum. The acoustic impedance mismatch in each interface causes reflection to take place at that interface. The degree to which they are reflected and transmitted is completely determined by the impedance variation along the two media.

However, real drill strings are not homogeneous or exactly periodic. The bottom-hole assembly contains elements of different dimensions and materials (for instance, some parts can be made of rubber or aluminum) [13]. Drill pipes can be formed of sections with different types of tool joints and may have different lengths. In practice, the pipe body may not be exactly uniform due to manufacturing tolerance and wear. There may

Manuscript received October 8, 2012; revised March 26, 2013 and September 23, 2013; accepted January 14, 2014. Date of publication March 11, 2014; date of current version May 30, 2014. This work was supported by the Agency for Science, Technology and Research (A*STAR), Singapore.

L. S. Kumar, Y. L. Guan, and Y. H. Lee are with the School of Electrical and Electronic Engineering, Nanyang Technological University, Singapore 639798 (e-mail: lskumar@ntu.edu.sg; eylguan@ntu.edu.sg; eyhlee@ntu.edu.sg).

W. K. Han was with Nanyang Technological University, Singapore 639798 (e-mail: wkhan@ntu.edu.sg).

S. Sun is with the Institute for Infocomm Research (I^2R), Agency for Science, Technology and Research (A*STAR), Singapore 138632 (e-mail: sunsm@i2r.a-star.edu.sg).

Color versions of one or more of the figures in this paper are available online at http://ieeexplore.ieee.org.

Digital Object Identifier 10.1109/TGRS.2014.2306686

be also different types of pipes for mass distribution per unit length, often in the same drill string. However, the pipes, in many cases, can be approximated as a periodic system of individual elements each formed of an elongated body with the pipe joints (tool joints) at its ends. Drumheller explained [14] that the length of all joints is constant for different sections of the pipe; however, there is considerable variation in the length of pipes among different sections because the pipe length is not accurately controlled during the manufacture of drill pipes. The positions of pass bands and stop bands are decided by the pipe length of the drill string. If a drill string is assembled using two pipes with different lengths, the resultant response allows waves with frequencies located in pass bands common to both pipe lengths.

It is disclosed in [14] and [15] that the selection and arrangement of downhole pipes plays a vital role in improving the transmission efficiency of extensional waves transmitted through the drill string for acoustic telemetry, particularly in the high-frequency bands. The order in which the pipes between the transmitter and the receiver are arranged has a significant impact on minimizing the transmission loss of signal energy from the transmitter to the receiver. If the pipes are arranged either in ascending or descending order based on their lengths, then peaks (or phase shifts) from the individual pipe lengths are closer to each other, which increase the resultant energy transfer. Pipes are arranged in ascending (descending) order based on their lengths from the source (downhole end) to the receiver (surface) for the ascend-only (AO) [descend-only (DO)] pipe arrangement. Peaks in the random pipe arrangements are away from each other, which reduces the resultant peak amplitudes and energy transfer. Random pipe arrangements spread the energy over a broad band of frequencies; echoes dispersed the waves and diluted the energy [14]. This is the reason for the selection of AO and DO pipe arrangements by Drumheller [14], [15].

It is found from the tapered dual-plane compact electromagnetic band gap microstrip filter structure [16] that ascending followed by the descending [ascend-then-descend (ATD)] arrangement exhibits wide and smooth pass band characteristics. In this pipe arrangement, peaks (or phase shifts) from the individual pipe lengths will be closer to one another as the pipes are either ascended or descended. In order to find the optimal pipe arrangement, in [17], four pipes with different lengths in increasing values between 8.8683 and 9.3434 m are arranged in all 24 possible permutations. The joint lengths are kept constant as 0.4751 m in [17], and it is concluded that placing the shortest and second shortest pipes at the downhole and surface ends of the drill string gives the optimal energy transfer. Therefore, ATD arrangement, one of the ordered pipe arrangements, which has the shortest and second shortest pipes at the downhole and surface ends of the drill string, is considered for analysis.

Another pipe arrangement, i.e., descending the pipes followed by ascending [descend-then-ascend (DTA)], is also considered for comparison. This pipe arrangement has smooth transition in pipe lengths from the first pipe to the last pipe, but it has the longest and second longest pipes at the downhole and surface ends of the drill string. In this paper, four ordered pipe arrangements, namely, AO, DTA, ATD, and DO, are considered. For illustrative purposes, five pipes of different lengths (values of lengths in increasing order), which are numbered as 1, 2, 3, 4, and 5, respectively, are arranged using AO by "12345," DTA by "53124," ATD by "13542," and DO by "54321." Pipes are arranged using these four ways starting from the source (downhole) to the receiver (surface). It is stated in [18] that signal attenuation is caused by various factors such as type of pipes, type of formation, well configuration, and density of the drilling fluid. Attenuation on drill string ranges between 4 and 7 dB/1000 ft for vertical to deviated wells under normal conditions. Therefore, attenuation of 7 dB/1000 ft (0.023 dB/m) is added in the finite-difference and transmission coefficient simulations.

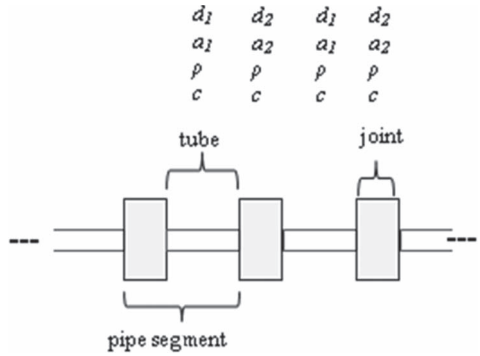

Fig. 1. Idealized drill string geometry.

Memarzadeh [19] stated that the high intensity of acoustic noise generated below 400 Hz prohibits the use of the first two pass bands for reliable communication, and on the upper end, 1800 Hz is the maximum acoustic frequency that can be generated by the transmitter's transducer. Therefore, energies are evaluated at the end of the drill string for different length drill strings from the frequency response found (third to sixth pass bands) using the transmission coefficients by arranging the pipes in the four ways considered. The study is extended up to 180 pipes. Extensional waves, which are less dispersive, as compared with bending and torsional waves [15], are selected as a means for communicating information from downhole to the surface.

II. Drill String Acoustic Channel

A. Finite-Difference Algorithm

The drill string can be seen as a slender elastic rod, which consists of a number of segments. The idealized drill string geometry is shown in Fig. 1. As shown in Fig. 1, each pipe segment has two types of elements—pipe and tool joint. The length of the element is d, the mass density is ρ, the cross-sectional area is a, and the velocity of the extensional waves is c. The acoustic wave propagation in the drill string is analyzed using the finite-difference algorithm [6], [17]. Assume that the position along the drill string is denoted by x and that time is denoted by t. The mass coordinate is defined as

$$m = \int_0^x \rho(\zeta) a(\zeta) d\zeta \tag{1}$$

TABLE I
DRILL STRING PARAMETERS

Element	d (m)	ρ (kg/m^3)	c (m/s)	a (m^2)
Tool joint	d_2=0.4751	7870	5130	a_2=16.2x10^{-3}
Pipe	d_1=9.1851			a_1=3.39x10^{-3}

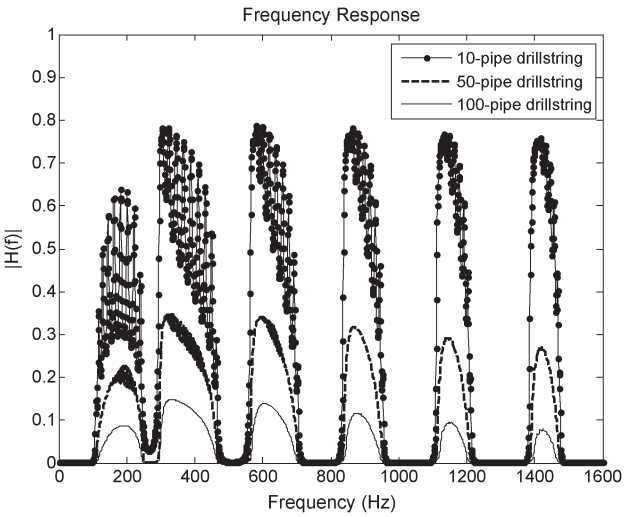

Fig. 2. Frequency response of constant pipe length drill strings.

and the impedance $z = \rho ac$. The extensional wave equation can be deduced as [6]

$$\frac{\partial^2 u}{\partial t^2} = \frac{\partial}{\partial m}\left(z^2 \frac{\partial u}{\partial m}\right). \tag{2}$$

The wave equation (2) is discretized, and the finite-difference algorithm can be obtained as

$$u_n^{j+1} + u_n^{j-1} = \frac{2\Delta r_{n+1/2}}{\Delta r_{n+1/2} + \Delta r_{n-1/2}} u_{n+1}^j + \frac{2\Delta r_{n-1/2}}{\Delta r_{n+1/2} + \Delta r_{n-1/2}} u_{n-1}^j \tag{3}$$

where u_n^j denotes the displacement field $u(x,t)$ at position $x = x_n$ and time $t = j\Delta t$, and n and j are the position and the time, respectively, $\Delta r_{n+1/2}$ denotes the string mass between the nth and the $(n+1)$th grids, being $\Delta r_{n+1/2} = \rho_{n+1/2} a_{n+1/2} \Delta x_{n+1/2}$.

Drill string parameters are listed in Table I. Drill strings consisting of 10 pipes (92 m), 50 pipes (458 m), and 100 pipes (915 m) are considered. For each of the drill string, tool joints are placed at the beginning and at the end of the drill string and placed between the pipes. An impulse excitation signal of time duration 30.87 μs is transmitted from the downhole, the wave displacement at the receiver is found for constant length 10-, 50-, and 100-pipe drill strings using finite-difference time-domain (FDTD) algorithm, and the corresponding frequency responses are plotted in Fig. 2. Signal attenuation of 7 dB/1000 ft is included in the simulations.

The values for ρ, a_1 (area of pipe), a_2 (area of joint), and c listed in Table I are used for all the simulations (Figs. 2, 4, and 5, Figs. 7(a) and (b)–9) in this paper. However, the values of d (d_1 is the length of pipe, and d_2 is the length of joint) in

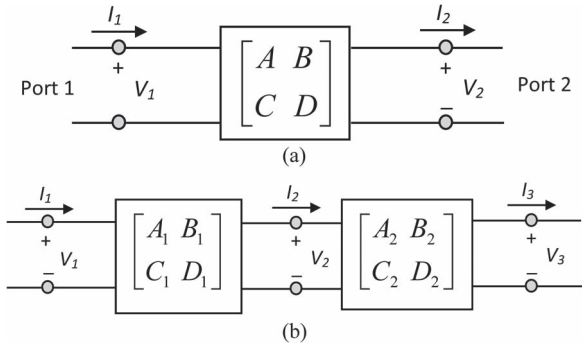

Fig. 3. Transmission matrix method. (a) Two-port network. (b) Cascaded connection of 2 two-port networks.

Table I are only used for Figs. 2 and 4. The values of d for the other figures are given in the following sections.

It is clear from Fig. 2 that the finite-difference simulations produce the familiar comb-filter-like channel response [6] expected for acoustic transmission along a metallic drill string with tool joints. The stop bands and pass bands result from destructive or constructive interference of reflected waves at different frequencies. Fig. 2 considers only segments of equal lengths. The drill string structure with N segments produces N spikes. In a drill string with 11 tool joints and 10 pipes, there are ten frequencies within the interior of each pass band, for which an integer number of half-wavelengths will fit into the total length of the string [6]. Resonances occur at each of these frequencies and manifest themselves as an individual spike in the pass band. As the length of the drill string increases, e.g., 915 m, for 100 pipes, spikes disappear in the smooth spectrum due to limited time window [6].

It is clear from Fig. 2 that the attenuation increases with the length and that the pass bands narrow. However, the positions of pass bands and stop bands are unchanged as the pass band beginnings (first peak) and stop bands/troughs in the pass band occur for $d_1 =$ multiples of $\lambda/2$ and $d_1 =$ multiples of $\lambda/4$, respectively. However, in practical operations, the lengths of the pipes are not constant, as mentioned in the introduction. If these variable pipe lengths are assembled for a drill string, the energy in the pass bands, particularly higher pass bands, is totally lost. To study the frequency responses of the variable length long drill strings, the transmission matrix method, which gives more precise and accurate results [20], [21], is included next.

B. Transmission Matrix Method

As shown in Fig. 1, the drill string is the structure of cascading joints and pipes alternatively. This is equivalent to the connection of cascaded two-port networks. Therefore, it is convenient to define a 2×2 transmission, or an $ABCD$ matrix, for each element or two-port network. The $ABCD$ matrix of the cascade connection of two or more two-port networks can be easily found by multiplying the $ABCD$ matrices of the individual two-port networks [22]. The voltages and currents on either side of the two-port network, as shown in Fig. 3(a), is related by

$$\begin{aligned} V_1 &= AV_2 + BI_2 \\ I_1 &= CV_2 + DI_2 \end{aligned} \tag{4}$$

or in matrix form as

$$\begin{bmatrix} V_1 \\ I_1 \end{bmatrix} = \begin{bmatrix} A & B \\ C & D \end{bmatrix} \begin{bmatrix} V_2 \\ I_2 \end{bmatrix}. \tag{5}$$

The transmission matrix for the lossy transmission line with the characteristic impedance Z_0 and length l is defined as

$$\begin{bmatrix} V_1 \\ I_1 \end{bmatrix} = \begin{bmatrix} \cosh(\gamma l) & Z_0 \sinh(\gamma l) \\ \sinh(\gamma l)/Z_0 & \cosh(\gamma l) \end{bmatrix} \begin{bmatrix} V_2 \\ I_2 \end{bmatrix} \tag{6}$$

where $\gamma = \alpha + j\beta$ is the complex propagation constant, α is the attenuation factor in nepers per meter, and $\beta = 2\pi/\lambda$ is the (real) propagation constant. Signal attenuation of 7 dB/1000 ft is converted into nepers per meter and is used as α in calculations. The relationship between the voltages and currents on either side of the cascaded connection of 2 two-port networks in Fig. 3(b) is given by

$$\begin{aligned} \begin{bmatrix} V_1 \\ I_1 \end{bmatrix} &= \begin{bmatrix} A_1 & B_1 \\ C_1 & D_1 \end{bmatrix} \begin{bmatrix} A_2 & B_2 \\ C_2 & D_2 \end{bmatrix} \begin{bmatrix} V_3 \\ I_3 \end{bmatrix} \\ &= \begin{bmatrix} A & B \\ C & D \end{bmatrix} \begin{bmatrix} V_3 \\ I_3 \end{bmatrix} = M_1 M_2 \begin{bmatrix} V_3 \\ I_3 \end{bmatrix} \end{aligned} \tag{7}$$

where the transmission matrix, i.e., M, of the cascaded connection of the two networks is equal to the product of the transmission matrices, i.e., M_1 and M_2, of the individual two-port networks. The transmission matrix of the tool joint (pipe), i.e., M_j (M_p), having the length d_2 m (d_1 m) and impedance $Z_j = \rho a_2 c$ ($Z_p = \rho a_1 c$) is defined by

$$\begin{aligned} M_j &= \begin{bmatrix} \cosh(\gamma d_2) & Z_j \sinh(\gamma d_2) \\ \frac{1}{Z_j} \sinh(\gamma d_2) & \cosh(\gamma d_2) \end{bmatrix} \\ M_p &= \begin{bmatrix} \cosh(\gamma d_1) & Z_p \sinh(\gamma d_1) \\ \frac{1}{Z_p} \sinh(\gamma d_1) & \cosh(\gamma d_1) \end{bmatrix}. \end{aligned} \tag{8}$$

As stated in Section II-A, tool joints are placed at the beginning and at the end of the drill string and placed between the pipes. The 2×2 transmission matrix for the variable length drill string with N pipes is calculated by

$$M = M_j M_{p1} M_j M_{p2} \ldots M_j M_{pN} M_j \tag{9}$$

where $M_{p1}, M_{p2}, \ldots, M_{pN}$ are the transmission matrices of the pipes with lengths $d_{11}, d_{12}, \ldots, d_{1N}$ respectively. The pipes (as well as the corresponding segments) are arranged from downhole to the surface end, and the transmission matrix is calculated accordingly. For convenience, the characteristic impedance of the drill string is set to the impedance Z_j of the joint pipe, yielding that all reflections are concentrated at the ends of the joints [23]. The transmission coefficient, i.e., S_{21} or T, of the drill string is calculated using the transmission matrix found from (9), i.e.,

$$T = \frac{2}{A + B/Z_j + CZ_j + D} \tag{10}$$

where Z_j is the characteristic impedance of the drill string.

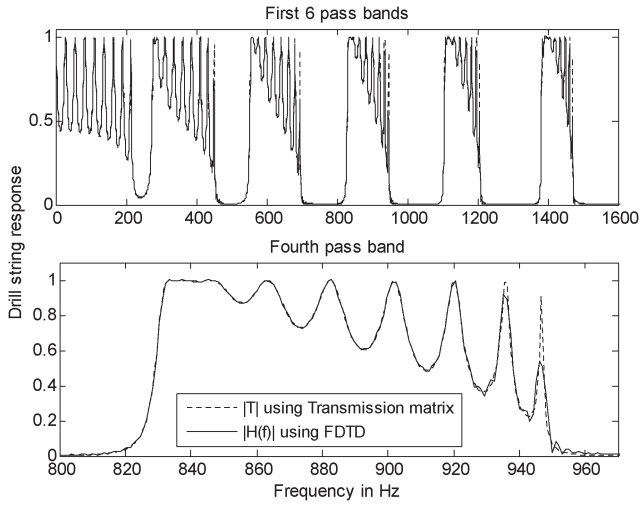

Fig. 4. Frequency response for the nine-pipe drill string using FDTD and transmission matrix methods.

III. Results and Discussion

A. FDTD and Transmission Matrix Response

The drill string parameters, which are given in Table I, are used to calculate the frequency responses for the drill string with nine pipes and ten tool joints, from FDTD and from transmission matrix using (3) and (10), respectively. Fig. 4 (subplots 1 and 2) shows the drill string response using the numerical (FDTD) and analytical (transmission matrix) methods for the first six pass bands and in the fourth pass band, respectively. Signal attenuation of 7 dB/1000 ft is not included in Fig. 4. As shown in Fig. 4, both methods have provided the comb-filter response and match well with each other. However, the spectrum obtained from the transmission matrix method is smooth and gives maximum gain (complete transmission) [20], as shown in Fig. 4 (subplot 2), at the peaks at around 935.5 and 946.5 Hz. FDTD is a numerical method, which calculates the displacement in discrete points and needs fast Fourier transform to find the frequency response from the impulse response. For the discretization, FDTD requires the ratio [6]

$$R = \frac{d_1/c}{d_2/c} = \frac{n_1}{n_2} \tag{11}$$

where d_1 and d_2 are the pipe and tool joint lengths in meters, respectively; c is the wave speed in meters per second; and n_1 and n_2 are the number of positions in the pipe and tool joint, respectively. The time interval Δt is selected using [15],

$$\begin{aligned} d_1 &= n_1 c \Delta t \\ d_2 &= n_2 c \Delta t. \end{aligned} \tag{12}$$

Pipes and tool joints use the equal position interval Δx. In Section II-A, the value of $\Delta t = 30.87$ μs resulting, d_1 (9.1851 m) has 58 positions, d_2 (tool joint) has three positions, and $\Delta x = 0.1584$ m. This restricts the difference between the two successive pipe lengths as 0.1584 m. Therefore, only few pipe lengths, which are multiples of 0.1584 m, can be selected within the practical pipe length range (8.8–10 m) and used for simulations. In practical drilling conditions, the drill string length is longer than 1 km; pipes are closer in length than

0.1584 m. It is necessary to consider more number of pipes with less deviation in length to find the optimal pipe arrangement. The minimum possible length difference of 0.1584 m is used in the finite-difference algorithm for Figs. 2 and 4. If this length difference is further reduced to include more pipes with length differences as low as 0.01 m by reducing Δt, then FDTD needs to work for more grids and introduces memory problems during simulations. FDTD's frequency resolution is limited to the sampling time, compared with the transmission matrix method. Moreover, the transmission matrix method is simple and produces more precise response [20], [21]. Therefore, it is used for further analysis to find the optimal pipe arrangement using more pipes; random pipe lengths with mean, i.e., μ, of 9.45 m and standard deviation, i.e., σ, of 0.16 m are considered to match with practical drill pipe lengths [15], [24]; tool joint length is fixed as 0.5 m.

As ordering these pipes improves the energy performance and decreases the attenuation, four different ordered pipe arrangements are considered. The AO and DO pipe arrangements are included for analyzing the energy performance of the drill string using more pipes. Ascending the pipes followed by descending (ATD) arrangement satisfies both the conditions required for the higher energy transfer, ordering the pipes based on their length, placing the shortest and second shortest pipes at the downhole and surface ends of the drill string. Therefore, the ATD arrangement is included for analysis. Another pipe arrangement, i.e., descending the pipes followed by ascending (DTA) is also considered for comparison. DTA pipe arrangement has smooth transition in pipe lengths from the first pipe to the last pipe, but it has the longest and second longest pipes at the downhole and surface ends of the drill string. The pipe arrangements AO, DTA, ATD, and DO are compared for 20-pipe drill string,and the frequency responses in the fourth pass band for different arrangements are analyzed next.

B. Pass Band Response for Different Pipe Arrangements

Pipes are arranged in ascending (descending) order from shortest (longest) to longest (shortest) for AO and DO pipe arrangements. For the DTA and ATD pipe arrangements, pipes are ordered based on the length; then, odd and even numbers of pipes are found. Even (odd) numbers of pipes are arranged in descending (ascending) order for half of the drill string length; then, odd (even) numbers of pipes are arranged in ascending (descending) order until the end of the drill string length for DTA (ATD) pipe arrangement. Fig. 5 shows the frequency response of the 20-pipe drill string in the fourth pass band using the AO, DTA, ATD, and DO pipe arrangements, respectively.

It is clear from Fig. 5 that the AO and DO pipe arrangements have given the same pass band response. This is because the drill string is a passive network. Fig. 6 shows the drill string with two pipes (pipe 1 and pipe 2) interconnected by joints. Fig. 6 is included to show that the drill string is the interconnection of joint and pipe impedances. As shown in Fig. 6, extensional waves are transmitted from the source (downhole end) through the drill string and received across the load (surface). For the AO pipe arrangement, the pipes are connected from shortest to longest from the source to the receiver. By

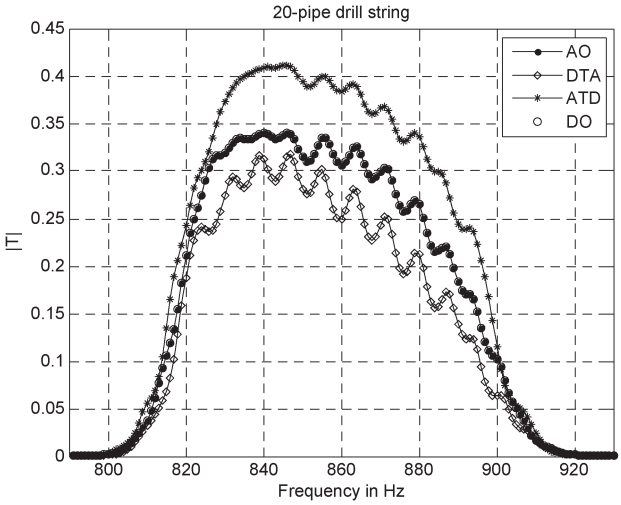

Fig. 5. Frequency response of the 20-pipe drill string in the fourth pass band.

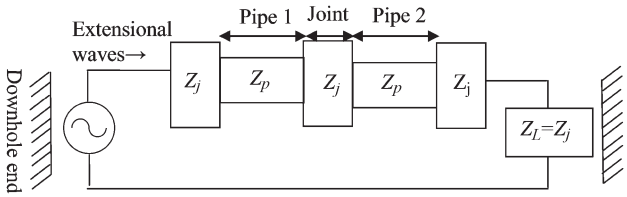

Fig. 6. Two-pipe drill string as an interconnection of two impedances.

interchanging the source and the receiver, the DO arrangement is obtained. As the drill string is a reciprocal network, the same response is obtained from the AO and DO pipe arrangements.

It is interesting to see from Fig. 6 that the ATD pipe arrangement has the higher and the wider pass band response, as compared with the other pipe arrangements. This is because of the relatively smooth transition in phase shifts from one pipe to another, and it also has the shortest and second shortest pipes at the downhole and surface ends of the drill string. In this arrangement, the impedance seen from the beginning and the end of the drill string is comparable, and both sides experience similar phase shifts, which makes the drill string to behave as the matched element between the input and output sides of the drill string. The response of the DTA pipe arrangement shows that it has the least and narrow pass band response, as compared with the other pipe arrangements. Although DTA has the ordered arrangement of pipes, the placement of the longest and second longest pipes at the downhole and surface ends of the drill string narrows the pass bandwidth and reduces the gain. AO and DO pipe arrangements produce higher gain, followed by the ATD pipe arrangement. As AO and DO pipe arrangements provide the same response, AO, DTA, and ATD pipe arrangements are considered for 20-, 40-, 80-, and 180-pipe drill strings; normalized received energy per subcarrier in the pass band is calculated and compared to find the optimal pipe arrangement next.

C. Optimal Pipe Arrangement

Fig. 7(a) shows the pipe length distributions for the three considered pipe arrangements. Random string of pipe lengths generated from MATLAB is included in Fig. 7(a) (subplots 3 and 4) for 80- and 180-pipe drill strings, respectively, denoted

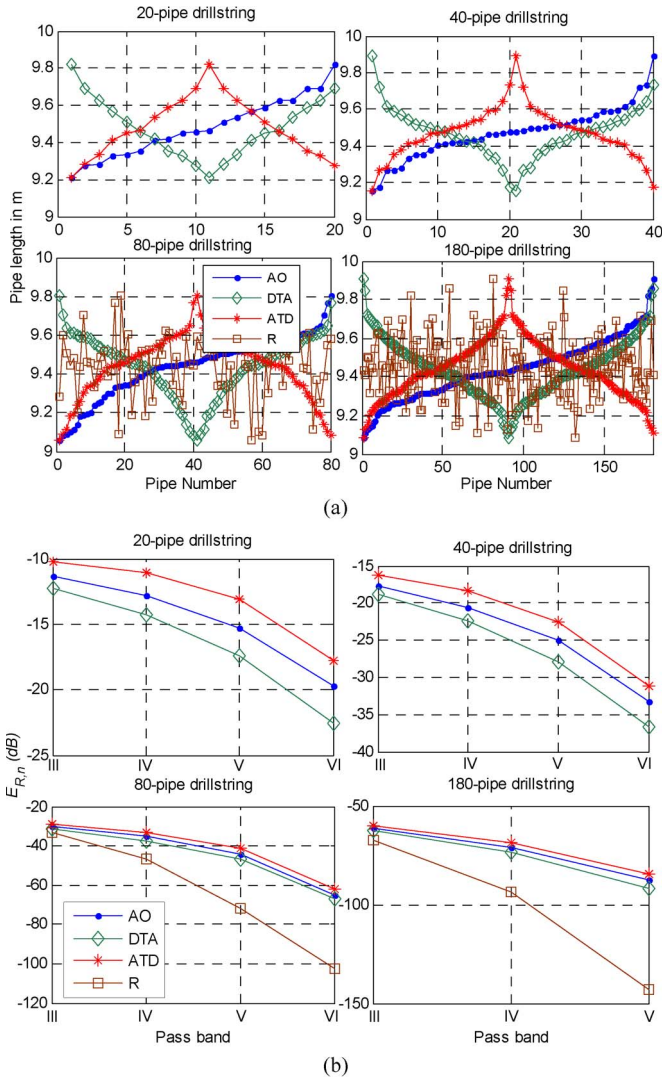

Fig. 7. (a) Pipe length distribution for 20-, 40-, 80- and 180-pipe drill strings. (b) Energy in decibels versus pass band comparison for different pipe drill strings.

by R in the legend in Fig. 7(a) and (b). As shown in Fig. 7(a), 20, 40, 60, and 180 pipes are arranged in AO, DTA, and ATD orders; and transmission coefficients are calculated for all the pipe arrangements using (9). Legend in subplot 3 is applicable to all the subplots in Fig. 7(a). Normalized received energy per subcarrier, i.e., $E_{R,n}$, in decibels is calculated from the transmission coefficients using

$$E_{R,n} = \frac{E_{\mathrm{Tx}}}{E_I} = \frac{\Delta \sum_i |T_i|^2}{\Delta \sum_i S_i^2} = \mathrm{Mean} \sum_i |T_i|^2$$
$$E_{R,n}(\mathrm{dB}) = 10 \log_{10}(E_{R,n}) \tag{13}$$

where i ranges the frequencies from the beginning to the ending of the pass band, Δ is the difference between the two adjacent frequencies (bandwidth) considered, and $\Delta = 1$ Hz is used in simulations; E_{Tx} is the transmitted energy in the pass band, E_I is the input energy for the pass band, $|T_i|$ is the transmission coefficient in the ith frequency, and S_i is the incident signal strength. Incident signal strength of unit amplitude is used in simulations. $E_{R,n}$ (dB) values are evaluated at the end of the drill string for single measurement, where the drilling lengths are known in advance.

TABLE II
NORMALIZED RECEIVED ENERGY PER SUBCARRIER IN PERCENT

Drill string size	$E_{R,n}$(%) (3rd to 6th pass bands		
	AO	DTA	ATD
20-pipe	70.03	50.56	100.00
40-pipe	65.92	46.50	100.00
80-pipe	70.20	48.39	100.00
180-pipe	71.23	51.87	100.00

1) Single Measurements: Fig. 7(b) (subplots 1–4) shows the $E_{R,n}$ (dB) values from the third to sixth pass bands for 20-, 40-, 80-, and 180-pipe drill strings, respectively. It is clear from Fig. 7(b) that the trend of the energy transfers gives comparable performances for different pipe arrangements from the third to sixth pass bands. The difference in the transferred energy is slightly higher in the fifth and sixth pass bands for different pipe arrangements. The ATD and AO pipe arrangements have more efficient energy transfer than the DTA and R pipe arrangements. The ATD pipe arrangement consistently gives around 1–4 and 3–7 dB higher energy than the AO and DTA pipe arrangements, respectively. The energy difference between different pipe arrangements increases with the length of the drill string, particularly at the higher pass bands. As shown in Fig. 7(b), for 20-pipe drill string, in the fifth pass band, the ATD pipe arrangement has 2.2 and 4.3 dB higher energy transfer than the AO and DTA pipe arrangements, respectively. However, for 180-pipe drill string, in the fifth pass band, the ATD pipe arrangement has 3.2, 7.3, and 58.5 dB higher energy transfer than the AO, DTA, and R pipe arrangements, respectively.

Random arrangement of drill pipes, i.e., R, gives poor performance, particularly at the higher pass bands. Although the process for arranging the pipes is time consuming, the enhancement in energy, particularly in the higher pass bands, is significant, as shown in Fig. 7(b) (subplots 3 and 4). The ATD pipe arrangement has higher energy transfer compared with the R arrangement of around 4.5, 13.8, 31.2, and 40.5 dB for 80-pipe drill string, and differences increase to around 7.4, 24.9, 58.5, and 92.4 dB for 180-pipe drill strings in the third, fourth, fifth, and sixth pass bands, respectively. Therefore, this paper recommends the use of ordered pipe arrangements compared with the random connection of pipes. Preprocessing of the pipes by labeling them based on the varying lengths the day before will speed up the drilling process. The use of pipe arrangements enhances the energy transfer in the third to sixth pass bands, thereby increasing the usable bandwidth for data transmission. The increased data rate increases the efficiency of the drilling process.

Table II shows the normalized received energy per subcarrier in percent $E_{R,n}$ (%) from the third to sixth pass bands using the three pipe arrangements for the drill strings considered. It is clear from Table II that the ATD pipe arrangement has more efficient energy transfer around 100% of the maximum value than the other pipe arrangements in the four pass bands (third to sixth) considered. For 180-pipe drill string, the R pipe arrangement transfers the least energy, around 16% of the maximum value, and the AO and DTA pipe arrangements transfer around 71% and 52% of the maximum value, respectively.

Although all the three pipe arrangements considered have smooth transition in the pipe lengths, the placement of the shortest and second shortest pipes at the beginning (downhole end) and at the end (surface) widens the pass band and increases energy transfer for ATD pipe arrangement. The ATD pipe arrangement has the higher energy transfer at all the pass bands for the considered drill strings. The AO pipe arrangement closely follows this pipe arrangement. The impedance matching at the two ends of the drill string enhances the energy transfer of the ATD pipe arrangement compared with the AO pipe arrangement. For the ATD pipe arrangement, impedance and phase shifts seen from the beginning and the end of the drill string are almost the same. This makes the drill string behave like an impedance-matched element between the acoustic transmitter and receiver. Although, for the DTA pipe arrangement, the impedance at the two ends of the drill string is matched, the placement of the longest and second longest pipes at the downhole and surface ends of the drill string reduces the energy performance of this arrangement less than it does for the ATD and AO pipe arrangements.

It is assumed in [10] that acoustic telemetry can tolerate a total loss of -50 dB in signal strength from the transmitter to the surface receiver. It is also assumed in [10] that, for a more severe loss of -60 dB, acoustic telemetry can still work at a reduced data rate. For 80-pipe drill string, loss in signal strength is still above -50 dB at the third, fourth, and fifth pass bands if the AO and ATD pipe arrangements are used. It is clear from Fig. 7(b) that the use of the ATD pipe arrangement enhances energy in the sixth pass band around -60 dB and makes that pass band usable for 80-pipe drill string. For 180-pipe drill string, the ATD pipe arrangement enhances energy in the third pass band around -60 dB and makes that pass band usable. Although the ATD pipe arrangement consistently gives higher energy than the R and other two ordered pipe arrangements, the other pass bands have lower gain less than -60 dB. In such situations, increasing the input gain or the use of repeaters may be helpful.

ATD pipe arrangement provides optimal performance for drill strings having pipe lengths with $\mu = 9.45$ m and $\sigma = 0.16$ m. In order to check the energy performance for other randomized drill strings, new pipes having $\sigma = 0.16$ m [another randomized string, which is different from the one shown in Fig. 7(a) and (b)] and $\sigma = 0.18$ m lengths are selected. The value of μ is kept constant as 9.45 m. Fig. 8 (subplots 1 and 2) shows the energy in decibels versus pass band comparison with pipe lengths having $\sigma = 0.16$ m and $\sigma = 0.18$ m for 80- and 180-pipe drill strings, respectively. It is clear from Fig. 8 that for 80- and 180-pipe drill strings with pipe lengths having $\sigma = 0.16$ m, the energy enhancement is seen for the ATD pipe arrangement from the third to sixth pass bands. The ATD pipe arrangement provides higher energy transfer around 2 dB, 3 dB in the sixth pass band, compared with AO pipe arrangement for 80- and 180-pipe drill strings when $\sigma = 0.16$ m. The trend of energy transfer is similar for different pipe arrangements, and energy enhancement is still there for ATD arrangement in Fig. 8, if $\sigma = 0.18$ m is used for pipe length generations. However, for 80-pipe drill string, having pipe lengths with $\sigma = 0.18$ m, as shown in Fig. 8 (subplot 2), energy in the sixth pass band reduces for all the pipe arrangements less than -60 dB.

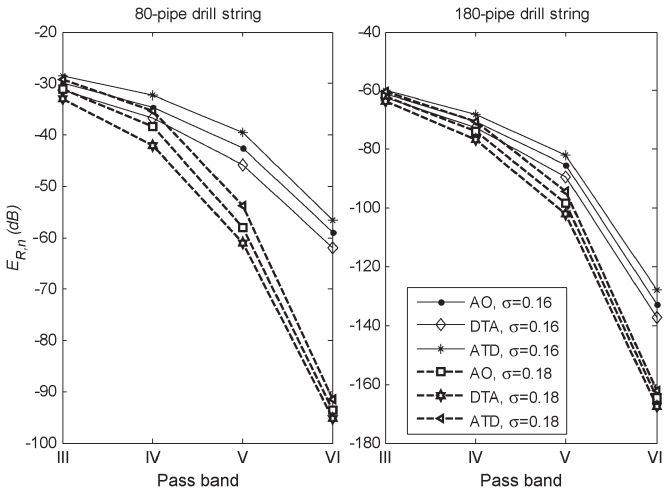

Fig. 8. Energy in decibels versus pass band comparison for 80- and 180-pipe drill strings with pipe lengths having $\sigma = 0.16$ m and $\sigma = 0.18$ m.

It is concluded from Fig. 8 that the optimal energy performance is provided by the ATD pipe arrangement for drill strings having pipe lengths with $\mu = 9.45$ m and $\sigma \leq 0.16$ m in the third to sixth pass bands and with $\mu = 9.45$ m and $\sigma \leq 0.18$ m in the third to fifth pass bands for 80-pipe drill string. Increasing the length deviations higher than 0.16 m reduces the usable energy in the sixth pass band less than -60 dB for 80-pipe drill string. In these situations, the third to fifth pass bands are usable, where the ATD pipe arrangement provides higher energy transfer compared with the other three pipe arrangements considered. The same analysis is applicable for 180-pipe drill string, except that the amount of energy transfer is lower than -60 dB in the fourth to sixth pass bands.

Energy comparisons in Figs. 7(b) and 8 are plotted for single measurement. However, the number of drill pipes used is not known in advance while drilling. In practical situations, it is necessary to vary the drill string length based on the oil's location by adding more pipes. For example, the 80-pipe drill string described earlier in Fig. 7(a) and (b) (subplot 3) uses one set of 80 pipes, and to include other set of 80 pipes (another random string of 80 pipes with $\mu = 9.45$ and $\sigma = 0.16$), ATD and AO pipe arrangements are repeated for analysis. These two pipe arrangements are selected as they provide better energy performances in the four pipe arrangements considered for single measurement. The two pipe arrangements, i.e., two sets of AO (2xAO) and two sets of ATD (2xATD), are analyzed for multiple measurements next.

2) Multiple Measurements: AO and ATD pipe arrangements are repeated using two sets of random strings of 80 pipes with $\mu = 9.45$ and $\sigma = 0.16$, as shown in Fig. 9 (subplot 1). The 2xATD pipe arrangement looks like up–down reversed "W" shape. Energies are compared after 80 pipes (first measurement) and after 160 pipes (second measurement), as shown in Fig. 7(b) (subplot 3) and Fig. 9 (subplot 2), respectively, from the third to sixth pass bands for the two pipe arrangements considered. As shown in Fig. 7(b) (subplot 3), $E_{R,n}$ (dB) values after 80 pipes show that the ATD pipe arrangement gives 100%, whereas the AO pipe arrangement gives 70.2% energy transfer from the third to the sixth pass bands. Energy performance after 160 pipes in Fig. 9 (subplot 2) shows that

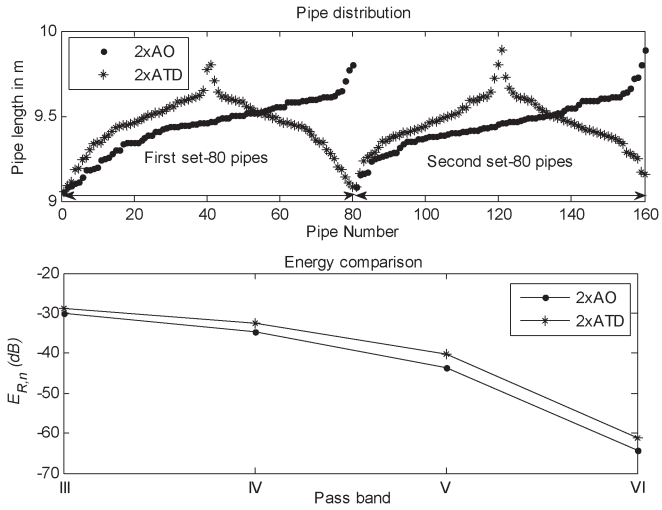

Fig. 9. (Subplot 1) Pipe length distribution for 160-pipe drill string. (Subplot 2) Energy in decibels versus pass band comparison for 160-pipe drill string. Two sets of 80 pipes are used for 160-pipe drill string.

the 2xAO pipe arrangement gives 70% energy transfer, whereas the 2xATD pipe arrangement has 100% energy transfer. The ATD pipe arrangement has higher energy transfer around 1.3, 2.1, 3.2, and 3.2 dB after 160 pipes in the third to sixth pass bands, respectively, than the AO pipe arrangement. As repeating the ATD pipe arrangement gives optimal performance for the measurements taken at the two points, after 80 and 160 pipes, the nxATD pipe arrangement is recommended for multiple measurements if the pipes come in sets.

For the case of two-way communication, the ATD and nxATD pipe arrangements exhibit maximum or near-maximum energy transfer compared with the other pipe arrangements considered. As shown in Figs. 7–9, the AO (nxAO) pipe arrangement, which is the closer competent for the ATD (nxATD) pipe arrangement, always gives 1–4 dB less energy per subcarrier in the pass bands considered. Therefore, the ATD and nxATD pipe arrangements are recommended as the optimal pipe arrangements to produce the best possible telemetry performance in terms of optimal acoustic energy transfer via one- and two-way acoustic communications for single and multiple measurements, respectively.

IV. Conclusion

Acoustic wave propagation in the downhole drill string geometry has been studied using the finite-difference algorithm and transmission coefficients. The resultant transfer function using the transmission coefficient simulations produces identical results similar to the finite-difference simulations. It is observed that the addition of segments increases the attenuation of the transmitted acoustic wave. If the pipe lengths have slight deviations, then arranging them based on the lengths improves the energy transfers. Four different pipe arrangements, which have smooth transitions in pipe lengths, namely, AO, DTA, ATD, and DO, are considered. Reciprocal nature of the drill string is tested and proved by providing same responses for AO and DO pipe arrangements. Normalized received energies per subcarrier $E_{R,n}$ in the pass bands are calculated and compared for different length drill strings using the transmission coefficients.

The use of ATD pipe arrangement consistently increases the energy transfer in the pass bands considered for single measurement. For 180-pipe drill string, the proposed pipe arrangement has 29% higher energy transfer (third to sixth pass bands) than the AO pipe arrangement (existed better pipe arrangement [14], [15]). The nxATD pipe arrangement is recommended in situations for multiple measurements if pipes are distributed in sets. For the case of two-way communication, both ATD and nxATD pipe arrangements exhibit maximum or near-maximum energy transfer compared with the other pipe arrangements considered. Therefore, ATD and nxATD pipe arrangements are recommended as best possible telemetry performance pipe arrangements in terms of optimal acoustic energy transfer for not only one-way but also two-way acoustic communication.

Acknowledgment

The authors would like to thank Dr. M. Je, A. A. Muthukumaraswamy, and W. Rajan of the Institute of Microelectronics, Agency for Science, Technology and Research (A*STAR) for their valuable suggestions. The authors would also like to thank the anonymous reviewers for their constructive comments and suggestions for this paper.

References

[1] N. C. MacLeod, "Apparatus and method for down-hole EM telemetry while drilling," U.S. Patent 4 739 325, Apr. 19, 1988.
[2] J. M. Carcione and F. Poletto, "A telegrapher equation for electric telemetering in drill strings," *IEEE Trans. Geosci. Remote Sens.*, vol. 40, no. 5, pp. 1047–1053, May 2002.
[3] G. Gould, "Optical communication system for drill hole logging," U.S. Patent 4 547 774, Oct. 15, 1985.
[4] M. S. Beattie and A. H. Abdnllah, "Mud pulse telemetry," U.S. Patent 6421298, Jul. 16, 1999.
[5] T. G. Barnes and B. R. Kirkwood, "Passbands for acoustic transmission in an idealized drill string," *J. Acoust. Soc. Amer.*, vol. 51, no. 5, pp. 1606–1608, 1972.
[6] D. S. Drumheller, "Acoustical properties of drill strings," *J. Acoust. Soc. Amer.*, vol. 85, no. 3, pp. 1048–1064, 1989.
[7] C. Li and T. Ding, "Signal wireless transmission behaviors along the drill string using extensional stress waves," in *Proc. IEEE ICIS*, 2010, pp. 541–545.
[8] T. H. Ali, J. A. Hood, S. R. Lemke, A. Srinivasan, J. McKay, C. Mondragon, S. C. Townsend, S. Edwards, K. S. Fereday, M. Hernandez, and M. Reeves, "High speed telemetry drill pipe network optimizes drilling dynamics and wellbore placement," in *Proc. Drilling Conf. IADC/SPE 112636*, 2008, pp. 55–63.
[9] L. Gao, W. Gardner, C. Robbins, M. Memarzadeh, and D. Johnson, "Limits on data communication along the drill string using acoustic waves," in *Proc. SPE Annu. Tech. Conf. Exhib.*, 2005, pp. 637–642.
[10] L. Gao, D. Finley, W. Gardner, C. Robbins, E. Linyaev, J. Moore, M. Memarzadeh, and D. Johnson, "Acoustic telemetry can deliver more real-time downhole data in underbalanced drilling operations," in *Proc. SPE/IADC Drilling Conf.*, 2006, pp. 485–490.
[11] V. H. Cox and P. E. Chaney, "Telemetry systems," U.S. Patent 4 293 936, Oct. 6, 1981.
[12] H. E. Sharp and I. A. Smither, "Borehole acoustic telemetry system with phase shifted signal," U.S. Patent 4 569 559, Dec. 31, 1985.
[13] F. Poletto and F. Miranda, "General theory: Drill-string waves and noise fields," in *Handbook of Geophysical Exploration: Seismic Exploration*, 3rd ed. Amsterdam, The Netherlands: Elsevier, 2004, ch. 4, pp. 163–212.
[14] D. S. Drumheller, "Downhole pipe selection for acoustic telemetry," U.S. Patent 5 477 505, Dec. 19, 1995.
[15] D. S. Drumheller, "Attenuation of sound waves in drill strings," *J. Acoust. Soc. Amer.*, vol. 94, no. 4, pp. 2387–2396, 1993.
[16] S. Y. Huang and Y. H. Lee, "Tapered dual-plane compact electromagnetic bandgap microstrip filter structures," *IEEE Trans. Microw. Theory Technol.*, vol. 53, no. 9, pp. 2656–2664, Sep. 2005.

[17] L. S. Kumar, W. K. Han, Y. L. Guan, S. Sun, Y. H. Lee, A. A. Muthukumaraswamy, and M. Je, "Downhole pipe selection and arrangement for acoustic drill string telemetry," in *Proc. 7th IEEE ICIEA*, 2012, pp. 1539–1542.
[18] L. Gao, W. Gardner, C. Robbins, D. Johnson, and M. Memarzadeh, "Limits on data communication along the drill string using acoustic waves," in *Proc. SPE Reservoir Eval. Eng.*, 2008, pp. 141–146.
[19] M. Memarzadeh, "Optimal borehole communication using multicarrier modulation," M.S. Thesis, Rice University, Houston, TX, USA, 2007.
[20] Y. W. Liu, Z. C. Guan, G. S. Zhao, and Z. Q. Long, "Discussion on commonly methods for analysis of drill string acoustic spectral characteristics," *Appl. Mech. Mater.*, vol. 226–228, pp. 466–469, 2012.
[21] C. Y. Wang, W. X. Qiao, and W. Q. Zhang, "Using transfer matrix method to study the acoustic property of drill strings," in *Proc. IEEE Int. Symp. Signal Process. Inf. Technol.*, 2006, pp. 415–419.
[22] D. M. Pozar, *Microwave Engineering*, 3rd ed. Hoboken, NJ, USA: Wiley, ch. 4, pp. 183–187.
[23] M. A. Gutierrez-Estevez, U. Krueger, K. A. Krueger, K. Manolakis, V. Jungnickel, K. Jaksch, K. Krueger, S. Mikulla, R. Giese, M. Sohmer, and M. Reich, "Acoustic broadband communications over deep drill strings using adaptive OFDM," in *Proc. IEEE WCNC*, 2013, pp. 4089–4094.
[24] D. S. Drumheller and S. D. Knudsen, "The propagation of sound waves in drill strings," *J. Acoust. Soc. Amer.*, vol. 94, pp. 2387–2396, 1995.

Lakshmi Sutha Kumar (M'13) received the B.Eng. degree from Bharathidasan University, Tiruchirappalli, India, in 1994, the M.Tech. degree from Vellore Institute of Technology, Vellore, India, in 2005, and the Ph.D. degree from Nanyang Technological University, Singapore, in 2012.

From 1995 to 1998 and from 1998 to 2002, she was a Lecturer with Bharathidasan University and Pondicherry University, Pondicherry, India, respectively. From 2011 to 2012, she was a Research Engineer with the School of Electrical and Electronic Engineering, Nanyang Technological University, where she has been a Research Fellow since 2012. Her research interests include microwave and millimeter-wave propagation, the study of the effects of rain on performance of microwave terrestrial and satellite communications, and channel characterization and modeling.

Wei Kwang Han received the B.Eng. degree in electrical and electronic engineering from Nanyang Technological University, Singapore, in 2003, and the M.Sc. degree in communications and signal processing and the Ph.D. degree in electrical and electronic engineering from Newcastle University, Newcastle upon Tyne, U.K., in 2005 and 2009, respectively.

From January 2011 to August 2011, he was an Electrical Engineer with Singapore PowerGrid. From September 2011 to August 2013, he was a Research Fellow with Nanyang Technological University, Singapore. His research interests include coded modulation, information theory, iterative receiver algorithms, error correction coding, diversity techniques, Orthogonal Frequency-Division Multiplexing (OFDM), statistical signal processing, and wireless communications.

Dr. Han is a member of the Institution of Engineering and Technology.

Yong Liang Guan (M'94) received the Bachelor's degree (with first-class honors) in engineering from the National University of Singapore and the Ph.D. degree from Imperial College London, London, U.K.

He is an Associate Professor and the Head of the Communication Engineering Division with the School of Electrical and Electronic Engineering, Nanyang Technological University, Singapore. His research interests include modulation and coding and signal processing for communication systems and information security systems.

Sumei Sun (SM'12) received the B.Sc. degree (with honors) from Peking University, Beijing, China, the M.Eng. degree from Nanyang Technological University, Singapore, and the Ph.D. degree from National University of Singapore, Singapore.

She has been with the Institute for Infocomm Research (I^2R), Agency for Science, Technology, and Research (A^*STAR), Singapore, where she is currently the Head of the Modulation and Coding Department, developing energy- and spectrum-efficient technologies for the next-generation communication systems. Her recent research interests include fifth-generation transmission technologies, renewable energy management and cooperation in wireless systems and networks, and wireless transceiver design.

Dr. Sun served as a Track Cochair for Mobile Networks, Applications, Services, IEEE Vehicular Technology Conference (VTC) 2014 Spring; a Track Cochair for Transmission Technologies, IEEE VTC 2012 Spring; the Technical Program Committee (TPC) Vice Chair for the 14th (2014) and the TPC Chair for the 12th (2010) IEEE International Conference on Communications; a General Cochair for the 7th (2010) and 8th (2011) IEEE Vehicular Technology Society Asia Pacific Wireless Communications Symposium; and a Track Chair for Signal Processing for Communications, Asia Pacific Signal and Information Processing Association Annual Summit and Conference 2010. She is an Editor of the IEEE TRANSACTIONS ON VEHICULAR TECHNOLOGY and an Editor of the IEEE WIRELESS COMMUNICATION LETTERS. She was a corecipient of the 16th Annual IEEE International Symposium on Personal Indoor and Mobile Radio Communications Best Paper Award.

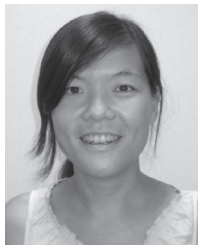

Yee Hui Lee (S'96–M'02) received the B.Eng. (Hons.) and M.Eng. degrees in electrical and electronics engineering from Nanyang Technological University, Singapore, in 1996 and 1998, respectively, and the Ph.D. degree from the University of York, York, U.K., in 2002.

Since July 2002, she has been an Associate Professor with the School of Electrical and Electronic Engineering, Nanyang Technological University. Her research interests include channel characterization, rain propagation, antenna design, electromagnetic band gap structures, and evolutionary techniques.